Mapping of strain and electric fields in GaAs/$Al_xGa_{1-x}As$ quantum-well samples by laser-assisted NMR

Marcus Eickhoff, Björn Lenzmann, and Dieter Suter
Universität Dortmund, Fachbereich Physik, D-44221 Dortmund, Germany

Sophia E. Hayes
Washington University, Department of Chemistry, St. Louis, Missouri 63130

Andreas D. Wieck
Ruhr-Universität Bochum, Angewandte Festkörperphysik, D-44780 Bochum, Germany
(Received 20 August 2002; revised manuscript received 5 November 2002; published 6 February 2003)

The usefulness of semiconductor heterostructures derives from the possibility to engineer their electronic and optical properties to match the requirements of many different applications. Optically detected nuclear magnetic resonance provides the possibility to map microscopic properties of such samples with a high spatial resolution through the splitting of resonance lines. In a multiple quantum-well sample, we measure the distortion of the crystal lattice and find variations of the order of 10^{-5} over distances of a few mm. Internal electric fields also cause resonance line splittings. Comparing the electric field-induced resonance line splittings in different quantum wells, we mapped the vertical variation of the electric field from a Schottky contact with a spatial resolution of some 40 nm.

DOI: 10.1103/PhysRevB.67.085308 PACS number(s): 73.30.+y, 76.70.Hb

I. INTRODUCTION

The combination of different semiconductor materials into heterostructure devices provides significant flexibility in adjusting electronic as well as optical properties of the resulting devices.[1] Epitaxial deposition of appropriate combinations of materials with different band gaps generates internal electric fields whose spatial variation yields the desired device properties. As a result of this design flexibility, such devices have found numerous applications in electronic and optoelectronic devices, such as lasers or photodetectors.

In addition to the band gap, the component materials also differ in their lattice constants. Accordingly, the resulting devices also include some degree of strain, whose magnitude depends on the lattice mismatch between the components. While strain may degrade the electronic or optical properties, controlled strain can also be used for modifying device properties, e.g., by shifting the emission wavelength of semiconductor lasers,[2] or by controlling the growth, such as for self-assembled InAs/GaAs quantum dots.[3]

The presence and spatial variation of strain can be measured with focused x-ray beams in grazing incidence with a spatial resolution of 1 μm^2.[4] This technique was also used to measure the strain distribution among periodically arranged quantum wires.[5] But with focused x-ray diffraction only distortions larger than a factor of 10^{-4} can be measured. In contrast to diffraction experiments, NMR spectroscopy is sensitive to local variations of lattice constants down to variations of less than 10^{-5}.[6] The distortion lowers the symmetry of the nuclear sites, thereby creating an electric-field gradient (EFG) that couples to the nuclear quadrupole moment of the $I=3/2$ spins ^{69}Ga, ^{71}Ga, and ^{75}As. As a result, the single transition frequency of the ideal cubic crystal splits into a triplet. The amount of splitting between these lines can be related directly to the lattice distortion.[6]

In a study by Sundfors,[7] components of the so called gradient-elastic tensor were determined from III-V single crystal semiconductors under elastic strain. Gradient-elastic proportionality constants, which determine the relationship between applied strain and electric-field gradients at the nucleus, were calculated for InSb and GaSb.[8] Bogdanov and Lemanov determined components of the *S* tensor (sometimes termed the "elastic compliance constants"), relating the EFG to elastic lattice deformation.[9]

Various sources contribute to internal electric fields in semiconductor heterostructures. Even in nominally undoped systems the difference of the energy levels between well and barrier materials forces the carriers to migrate from one material to another in order to equalize the difference in chemical potential. Furthermore, electrical contacts create additional fields in the form of a Schottky barrier: electrons are transferred to the metal, leaving ionized donor states in the neighboring semiconductor. Therefore, an electric field develops at the metal-semiconductor interface, which is a function of position within the sample in the "vertical" or growth direction (normal to the metal-semiconductor interface).

While homogeneous electric fields do not couple directly to the nuclear quadrupole moment, they distort the charge distribution at the nuclear sites, which do not have inversion symmetry. As a result, electric fields can also cause splittings of the nuclear spin transitions.[10] The coupling constant between the electric field and the EFG at the nuclear site has been determined for bulk GaAs by various groups.[10,11]

While earlier measurements of these effects in bulk GaAs were done with conventional magnetic resonance techniques, they are not sensitive enough for measurements on quantum confined structures. For such systems, optical pumping, often in combination with optical detection[12–14] is necessary for

 ©2003 The American Physical Society

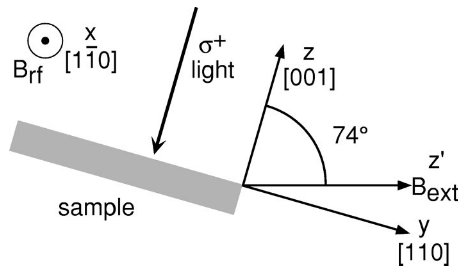

FIG. 1. The coordinate frame (x', y', z') is aligned to the external magnetic field B_{ext} and the (x, y, z) frame to the crystallographic axes of the sample. The incident laser light is parallel to the growth direction of the sample (z), and the radio frequency field B_{rf} is applied perpendicular to B_{ext}.

providing sufficient sensitivity and selectivity to perform measurements on single quantum films. Earlier studies of GaAs materials have used optically detected nuclear magnetic resonance (ODNMR) methods for studying defects,[15] the Overhauser shift,[16] magnetic g factor,[17,18] exciton spin relaxation,[19] response of the material to an ac electric field,[20] and fractional quantum Hall effect.[21,22] The presence of quadrupolar splittings was demonstrated by various groups.[23,24] It has been suggested that ODNMR is capable of resolving individual epitaxial layers.[25,26] In addition to quantum films, ODNMR has also been applied to quantum dots.[27–29] Here we use ODNMR to map lattice distortions and electrical fields in semiconductor heterostructures with a resolution in the μm to nm range.

II. SAMPLE AND EXPERIMENT

The experiments were performed on two identical pieces of a multiple quantum-well sample grown by molecular beam epitaxy (MBE) on a (001) oriented GaAs substrate. We align our coordinate system along the growth direction and the cutting edges of our sample, with the growth direction pointing in the z-direction and the x axis aligned with one of the [110] directions of the crystal (see Fig. 1). One of the pieces used in this study was coated with an indium tin oxide (ITO) layer on top of the sample to provide an electrical contact while the other was left uncoated. The thickness of the wells varied between 2.8 and 19.7 nm, and they were separated by 30.9 nm $Al_{0.3}Ga_{0.7}As$ barriers (see Fig. 2). The distance of each quantum well from the crystal surface was known from the MBE growth protocol. Five of the widest quantum wells (6.8, 10.5, 11.7, 14.5, and 19.7 nm) were in the range of the external cavity diode laser used for optical excitation. These quantum wells are at distances of 260 to 471 nm from the top surface.

For the measurements, the samples were glued with silver print to the cold finger of a continuous flow cryostat, which cooled the sample to temperatures of 4–7 K. The laser light used for excitation and optical pumping was focused to approximately 50 μm diameter and incident parallel to the growth axis of the sample, which was oriented by an angle of 74° with respect to the external magnetic field. If the light is circularly polarized, the photoexcited carriers are spin polarized, and a significant fraction of this polarization is transferred to the nuclear spin system.[30]

The photoluminescence (PL) emitted from the sample was collimated, passed through a photoelastic modulator (PEM) for polarization modulation and a spectrometer for wavelength selection, and detected with an avalanche photodiode. The degree of polarization of the light was determined by a lock-in amplifier, which was referenced to the PEM driver. The laser wavelength was set to the high energy side of the optical resonance line of the quantum well to be studied, and the spectrometer was set to the low-energy side of the same resonance line.

For the optical detection of NMR, a radio frequency (rf) field was applied by a coil perpendicular to the external magnetic field. If the resonance condition for the rf field and the nuclear transition frequency is met, the nuclear polarization is reduced, which can be detected as a change in the polarization of the photoluminescence emitted by the sample.[31] In the experiments described here, NMR spectra were measured at a fixed external magnetic field by scanning the radio frequency over the nuclear transition frequency.

Figure 3 shows a typical experimental spectrum from the 19.7 nm quantum well. For this spectrum only the nuclear

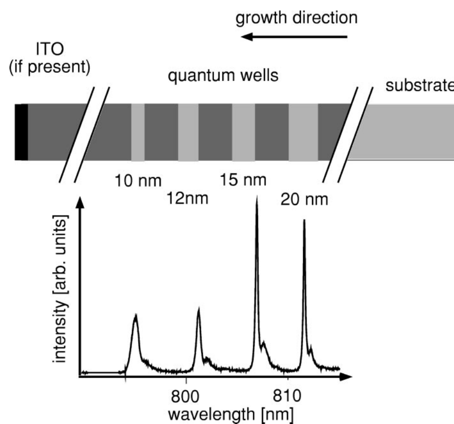

FIG. 2. The upper part shows a sketch of the sample with the AlGaAs and GaAs material symbolized by the dark and light grey areas, respectively. The lower part shows a PL spectrum with the appropriate quantum well placed directly above each resonance.

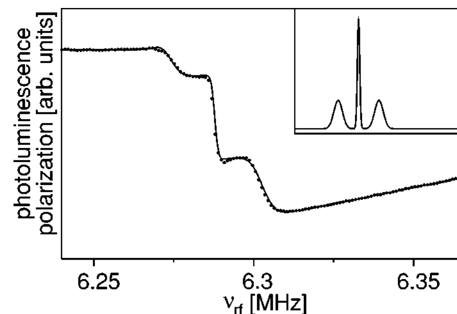

FIG. 3. Example of an ODNMR spectrum from the 19.7 nm quantum well. The dots indicate the experimental data. The solid curve represents the theoretical spectrum calculated with the following parameters: 15 kHz quadrupole splitting, 1.1 and 3.8 kHz half width at half maximum for the central and the satellite lines, respectively, and 130 mT width of the Hanle curve. The conventional NMR spectrum corresponding to these parameters is shown in the inset.

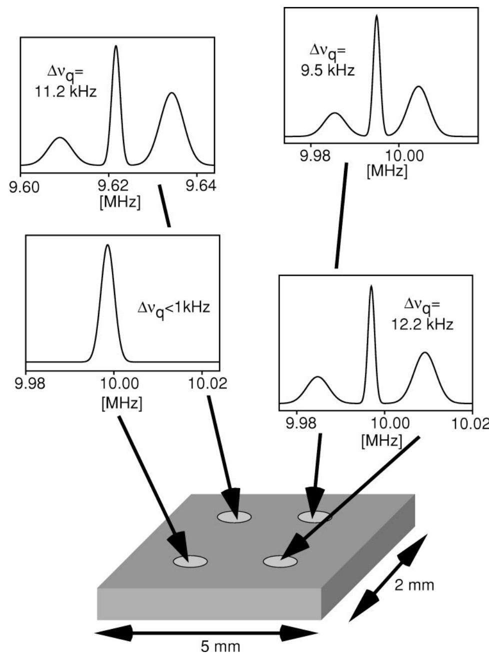

FIG. 4. Lateral change of quadrupole splitting. All spectra were recorded for a single quantum well of width 19.7 nm in an area smaller than 4 mm^2.

spins in a volume of cylindrical shape with the diameter of the laser focus and the height of the quantum well contribute to the signal. In this example, the magnetic field was set to 0.863 T, and the nuclear spins were optically pumped for 60 sec. After the nuclear polarization was established, the radio frequency was scanned from 6.240 to 6.365 MHz while the PL polarization was measured. Three distinct steps in the PL polarization can be attributed to the three resonances of the ^{75}As spins. A simulation of the spectrum (solid curve) agrees well with the experimental data points for the parameters given in the figure caption. Using the same parameters, we also calculated the conventional NMR spectrum, which is shown in the inset. The quadrupole splittings of both gallium isotopes are smaller than that of ^{75}As and were thus not investigated in this work.

III. LATERAL VARIATION

The splitting of the resonance lines by the interaction of the nuclear quadrupole moment with a strain-induced EFG has been investigated in bulk GaAs (Ref. 32) and GaAs quantum wells.[6,23,24] Guerrier and Harley[6] have calibrated the quadrupole splitting ν_q as a function of uniaxial strain ϵ by applying a well defined force to the sample, for which they found the linear relation $\epsilon = \nu_q \, 4.7\times 10^{-6}$ kHz^{-1}.

The quadrupolar splitting is thus a useful probe for the local strain in the sample. We measured a number of spectra at different positions in the sample. Figure 4 shows four such spectra which were measured in the 19.7 nm quantum well, at a depth of 471 nm from the top surface of the sample. In our experimental setup, the spatial resolution is limited by the diameter of the laser beam focused on the sample, whose diameter is on the order of 50 μm. For these spectra, the quadrupolar splitting varies from <1 kHz to 12.2 kHz (corresponding to $\epsilon < 4.7\times 10^{-6}$ and $\epsilon = 5.7\times 10^{-5}$, respectively) over an area of approximately 2 mm^2. The strain values are calculated for uniaxial stress in growth direction. They should only represent an order of magnitude for the strain in any direction in the sample.

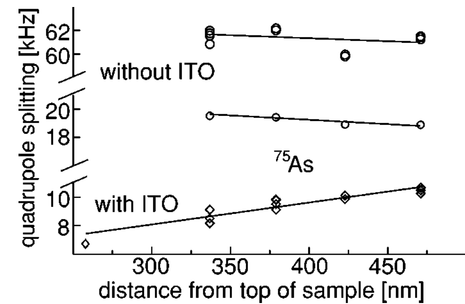

FIG. 5. Quadrupolar splittings of ^{75}As as a function of depth within the multiple quantum-well sample. The upper two sets were measured on a piece of the sample without an ITO layer on top, and the lower set was from a piece with an ITO layer on top. All three measurements were made at different positions on the sample.

At all positions measured in the uncoated sample, the quadrupole splittings depended only on the lateral position, not on the depth from the surface (see the upper two data sets in Fig. 5). This suggests that the strain gradient is very small in the vertical direction.

The observed variation of strain over the sample may originate from a number of sources, such as variability of the growth conditions or the substrate. An additional source associated with the experimental setup may be the mounting of the sample: the sample, support, and the silver print used for mounting the sample all have different thermal expansion coefficients. No attempt was made in this study to control these effects. All these sources may generate stress inside the sample pointing in arbitrary directions. Due to the tensor character of the coupling between quadrupolar splitting and strain, the observed quadrupolar splitting varies with the direction of the stress and its magnitude.

IV. DEPTH PROFILE

A typical source of electric fields is the Schottky barrier associated with the metal-semiconductor interface between the GaAs crystal and a surface electrode. Such electrodes are used in many device applications as well as in many experimental setups, where electric fields or injected carriers are required.

While the nuclear spin does not couple to a homogeneous electric field E it does interact with the EFG through the nuclear electric quadrupole moment Q. Since the nuclei in GaAs are located at positions that lack inversion symmetry, an electric field applied to the sample causes a distortion of the orbitals and nuclear structure in such a way that it induces quadrupole coupling.[10,11,20] This indirect coupling makes quadrupolar spins located at sites without inversion symmetry sensitive probes of electric fields. We use this fact to probe the electric field variation in a multiple quantum well sample.

On this sample, we measured NMR spectra whose lateral

position was defined by the laser beam position, while the vertical position was defined through the wavelength setting of the laser and the spectrometer. Figure 5 shows data taken from a series of ^{75}As NMR spectra that were measured at the same lateral position, but from different quantum wells and therefore at different depths in the sample. The quadrupole splittings marked by (○) were taken on the piece of sample without an ITO layer, and the measurements indicated by (◇) were taken on the piece capped with an ITO overlayer. While the quadrupolar splitting is almost constant as a function of depth in the uncapped sample, the sample with the overlayer shows a clear increase of the quadrupole splitting with depth.

This variation of the quadrupolar splittings appears to be superimposed to a constant background splitting caused by strain and can be rationalized with a simple model for the internal field generated by a Schottky barrier. The potential difference between GaAs or AlGaAs and a metal contact is about $V_b^{\mathrm{ITO}} \approx 1$ V.[33,34] The resulting accumulation of charges near the interface creates a potential barrier in the semiconductor that decreases quadratically with the distance z from the interface

$$V^{\mathrm{ITO}}(z)=V_b^{\mathrm{ITO}}\left(\frac{z-d}{d}\right)^2 \quad (\text{for } z<d), \tag{1}$$

where d is the width of the Schottky barrier. The electric field therefore decreases linearly with the distance from the interface

$$E^{\mathrm{ITO}}(z)=-\operatorname{grad} V^{\mathrm{ITO}}(z)=2V_b^{\mathrm{ITO}}\frac{d-z}{d^2}. \tag{2}$$

As discussed above, this electric field couples to the quadrupole moment. Writing the quadrupole interaction as

$$H_Q=\frac{eQ}{4I(2I-1)}V_{z'z'}(3I_{z'}^2-I^2), \tag{3}$$

where I is the nuclear spin, $I_{z'}$ its component along the external field direction, e the electron charge, V_{ij} the EFG matrix elements, and Q the quadrupole moment. Because of the symmetry of the sample, the electric field is aligned with the growth direction. The EFG is proportional to the electric field at the nuclear site

$$V_{ij}=C_{ij,k}E_k, \tag{4}$$

where $C_{ij,k}$ is the element of the coupling tensor, which relates the EFG to the electric field in the k direction E_k. If the electric and magnetic fields are both oriented along the [001] direction, the only relevant tensor element is $C_{xy,z}$. For ^{75}As, this coupling constant is approximately $C_{14}=3\times10^{12}\ \mathrm{m}^{-1}$, with the indices given in Voigt notation.[10,11]

In our setup, the magnetic field is oriented along the z' direction, which is tilted by $\theta=74°$ with respect to the growth direction (see Fig. 1). For such a rotation Brun *et al.*[35] calculated the whole coupling tensor. The only element generating an EFG by applying an electric field in growth direction is

$$C_{z'z',z}=3\sin^2\theta\cos\theta C_{14}=0.76C_{14} \quad (\text{for } \theta=74°). \tag{5}$$

According to Eq. (3), this EFG causes a quadrupole splitting. The observed quadrupole splittings of the narrowest and the widest quantum well, which are 210 nm separated from each other, differ by 3.2 kHz. This change of splitting corresponds to a change of the electric field of 390 kV/m over the same distance. According to Eq. (2), and assuming the Schottky voltage to be $V_b^{\mathrm{ITO}}\approx 1$ V, the thickness d of the Schottky barrier is approximately 1 μm. The expected thickness[36]

$$d=\sqrt{\frac{2\varepsilon\varepsilon_0|V_b^{\mathrm{ITO}}|}{ne}} \tag{6}$$

evaluates to ≈ 1 μm if we use the dielectric constant of GaAs, $\varepsilon=12.53$, and a carrier concentration of $n=1.3\times10^{15}\ \mathrm{cm}^{-3}$.

An electric-field contribution to the observed splittings cannot be excluded for the uncapped sample. Electric fields can be caused, e.g., by surface states causing band bending and carrier depletion. However, due to the nearly constant depth profile of the quadrupole splitting in the uncapped sample (see Fig. 5 upper two traces) such an influence seems to be quite small.

Similarly, the ITO layer may contribute to the mechanical strain in the sample. Such effects are not distinguishable from other sources of strain, and we estimate that its effect is negligible compared to those discussed here.

V. CONCLUSION

We have shown that ODNMR can be used to map the distribution of internal electrical fields and mechanical strain in GaAs / AlGaAs heterostructures. The strain can be measured with a precision of $\approx 10^{-6}$, while electrical fields can be measured with a resolution of ≈ 100 kV/m.

In our setup, we could map these interactions with a spatial resolution on the order of 50 μm in the lateral direction, limited by the diameter of the laser focus. Using tighter focusing, resolution could be increased to <1 μm.[37] In the vertical direction, the resolution is on the order of nanometers, limited by the width of the quantum wells.

We have shown that the observed resonance line splittings can be explained in terms of electric fields and mechanical strain. The separation into these two contributions is not straightforward with the present experimental setup. In addition, we only could quantify the strain with a scalar measure; it would be highly desirable to measure the full strain tensor instead. This goal may be achieved by rotating the magnetic field and therefore the direction onto which the quadrupole coupling is truncated. From such an orientation dependence, it should then be possible to determine all components of the strain tensor and to separate the effect of strain from those induced by electrical fields.

[1] H. Kroemer, Rev. Mod. Phys. **73**, 783 (2001).
[2] S. Simanowski, N. Herres, C. Mermelstein, R. Kiefer, J. Schmitz, M. Walther, J. Wagner, and G. Weimann, J. Cryst. Growth **209**, 15 (2000).
[3] H. Lee, J. A. Johnson, M. Y. He, J. S. Speck, and P. M. Petroff, Appl. Phys. Lett. **78**, 105 (2001).
[4] H. R. Lee, D. Kupperman, W. Yun, Z. Cai, and W. Rodrigues, Rev. Sci. Instrum. **70**, 175 (1999).
[5] V. M. Kaganer, B. Jenichen, G. Paris, K. H. Ploog, O. Konovalov, P. Mikulík, and S. Arai, Phys. Rev. B **66**, 035310 (2002).
[6] D. J. Guerrier and R. T. Harley, Appl. Phys. Lett. **70**, 1739 (1997).
[7] R. K. Sundfors, Phys. Rev. **177**, 1221 (1969).
[8] R. G. Shulman, B. J. Wyluda, and P. W. Anderson, Phys. Rev. **107**, 953 (1957).
[9] V. L. Bogdanov and V. V. Lemanov, Sov. Phys. Solid State **10**, 159 (1968).
[10] K. A. Dumas, J. F. Soest, A. Sher, and E. M. Swiggard, Phys. Rev. B **20**, 4406 (1979).
[11] D. Gill and N. Bloembergen, Phys. Rev. **129**, 2398 (1963).
[12] D. Paget, Phys. Rev. B **24**, 3776 (1981).
[13] J. A. Marohn, P. J. Carson, J. Y. Hwang, M. A. Miller, D. N. Shykind, and D. P. Weitekamp, Phys. Rev. Lett. **75**, 1364 (1995).
[14] J. M. Kikkawa and D. D. Awschalom, Science **287**, 473 (2000).
[15] S. K. Buratto, D. N. Shykind, and D. P. Weitekamp, Phys. Rev. B **44**, 9035 (1991).
[16] M. Krapf, G. Denninger, H. Pascher, G. Weimann, and W. Schlapp, Solid State Commun. **78**, 459 (1991).
[17] M. J. Snelling, G. P. Flinn, A. S. Plaut, R. T. Harley, A. C. Tropper, R. Eccleston, and C. C. Phillips, Phys. Rev. B **44**, 11 345 (1991).
[18] N. J. Traynor, R. T. Harley, and R. J. Warburton, Phys. Rev. B **51**, 7361 (1995).
[19] R. T. Harley and M. J. Snelling, Phys. Rev. B **53**, 9561 (1996).
[20] J. G. Kempf and D. P. Weitekamp, J. Vac. Sci. Technol. B **18**, 2255 (2000).
[21] R. L. Brockbank, H. D. M. Davies, J. F. Ryan, M. A. Thomson, and A. J. Turberfield, Physica E **6**, 1 (2000).
[22] H. D. M. Davies, R. L. Brockbank, J. F. Ryan, and A. J. Turberfield, Physica B **258**, 104 (1998).
[23] M. Schreiner, H. Hochstetter, H. Pascher, and S. A. Studenikin, J. Mater. Res. **124**, 80 (1997).
[24] M. Schreiner, H. Pascher, G. Denninger, S. A. Studenikin, G. Weimann, and R. Lösch, Solid State Commun. **102**, 715 (1997).
[25] S. K. Buratto, D. N. Shykind, and D. P. Weitekamp, J. Vac. Sci. Technol. B **10**, 1740 (1992).
[26] S. W. Brown, T. A. Kennedy, E. R. Glaser, and D. S. Katzer, J. Phys. D **30**, 1411 (1997).
[27] S. W. Brown, T. A. Kennedy, and D. Gammon, Solid State Nucl. Magn. Reson. **11**, 49 (1998).
[28] D. Gammon, A. L. Efros, T. A. Kennedy, M. Rosen, D. S. Katzer, D. Park, S. W. Brown, V. L. Korenev, and I. A. Merkulov, Phys. Rev. Lett. **86**, 5176 (2001).
[29] S. I. Erlingsson, Y. V. Nazarov, and V. I. Fal'ko, Phys. Rev. B **64**, 195306 (2001).
[30] Optical Orientation, edited by F. Meier and B. P. Zakharchenya (North-Holland, New York, 1984).
[31] M. Eickhoff, B. Lenzman, G. Flinn, and D. Suter, Phys. Rev. B **65**, 125301 (2002).
[32] W. E. Carlos, S. G. Bishop, and D. J. Treacy, Phys. Rev. B **43**, 12 512 (1991).
[33] N. Blasubramanian and D. Subrahmanyam, Thin Solid Films **193/194**, 528 (1990).
[34] P. Revva, J. M. Langer, M. Missous, and A. R. Peaker, J. Appl. Phys. **74**, 416 (1993).
[35] E. Brun, R. J. Mahler, H. Mahon, and W. L. Pierce, Phys. Rev. **129**, 1965 (1963).
[36] Ch. Kittel, *Introduction to Solid State Physics, 6th ed.* (Wiley, New York, 1986).
[37] J. Kasai and Y. Katayama, Rev. Sci. Instrum. **66**, 3738 (1995).